JOURNAL OF MATERIALS SCIENCE 33 (1998) 5873–5881

Mechanical alloying of immiscible Pb-Al binary system by high energy ball milling

M. ZHU§, X. Z. CHE, Z. X. LI
Department of Mechano-Electronic Engineering, South China University of Technology Guangzhou 510641 P.R. China
E-mail: memzhu@scut.edu.cn

J. K. L. LAI
Department of Physics and Materials Science, City University of Hong Kong, 83 Tat Chee Avenue, Kowloon, Hong Kong

M. QI
Department of Materials Engineering, Dalian University of Technology, Dalian 116023 P.R. China

In the present work, mechanical alloying has been applied to the Pb-Al immiscible binary system by using the method of high energy ball milling. The microstructural features of the milled powder, such as grain size, lattice constant and morphology of phases have been studied by X-ray diffraction, analytical transmission electron microscopy (TEM) and scanning electron microscopy (SEM). Besides, energy dispersive spectroscopy was used to analysis chemical composition of phases presented after milling. Differential Scanning Calorimetry measurement was also made on the milled Pb-Al powder. The results show that homogenous blending of Pb and Al can be easily achieved by high energy ball milling in spite of their mutual immiscibility and large difference in density. The obtained alloy exhibits nanocrystalline microstructure. Further more, the experiment result implies the formation of supersaturated solid solution in immiscible Pb-Al system by high energy ball milling.

1. Introduction

Since Yermakov [1] and Koch [2] reported the preparation of amorphous metals by high energy ball milling (HEBM), the novel method of mechanical alloying (MA) using HEBM as the main technique has been widely used to synthesize various advanced materials. As a result, a broad range of non-equilibrium phase transformation and chemical reactions have been observed in the process of MA in a wide variety of systems including metal-metal, metal-oxide, ceramics and so on. Alloys, intermetallic compounds, ceramics and composites can be prepared in the amorphous or nanocrystalline state [3]. In recent years, the formation of supersaturated solid solutions by HEBM has been achieved in many cases, such as Zr-Al alloy [4], AlCo intermetallic compound [5] and ZrO_2-CeO_2 ceramic system [6]. One of the most unusual effects is the formation of nanocrystalline non-equilibrium solid solution for alloys, e.g., Ag-Cu [7], Cu-Hg [8] and Fe-Cu [9], which are virtually immiscible under thermodynamic equilibrium conditions due to their positive enthalpy of mixing. The supersaturated solid solutions obtained in immiscible systems have shown some unique properties. For example, apparent softening and strengthening effects have been observed with the increase of solute concentrations in Fe-Cu nanocrystalline supersaturated solid solution and Fe-Cr nanocrystalline solid solution respectively [10]. Magnetic measurement has also shown some interesting magnetic properties for Fe-Cu nanocrystalline supersaturated solid solutions [11].

The driving force and mechanism for the formation of supersaturated solid solution have been attributed to several aspects. With respect to the formation of nanocrystalline supersaturated solid solution in Ag-Fe immiscible system by inert gas condensation, Herr *et al*. suggested that the dissolution was located mainly in the boundary region [12]. This mechanism was also used to explain the formation of nanocrystalline AlCo phase supersaturated with Al prepared by ball milling [5]. According to the estimation of free energy change as the structure refined by mechanical attrition in the Fe-Cu system, it was suggested that capillary pressure of fine particles may provide the driving force for the dissolution of one component into another [13]. It has also been proposed that the stress field of dense dislocations produced by the severe deformation of MA is responsible for the formation of supersaturated solid solution [14].

§ Author to whom all correspondence should be addressed.

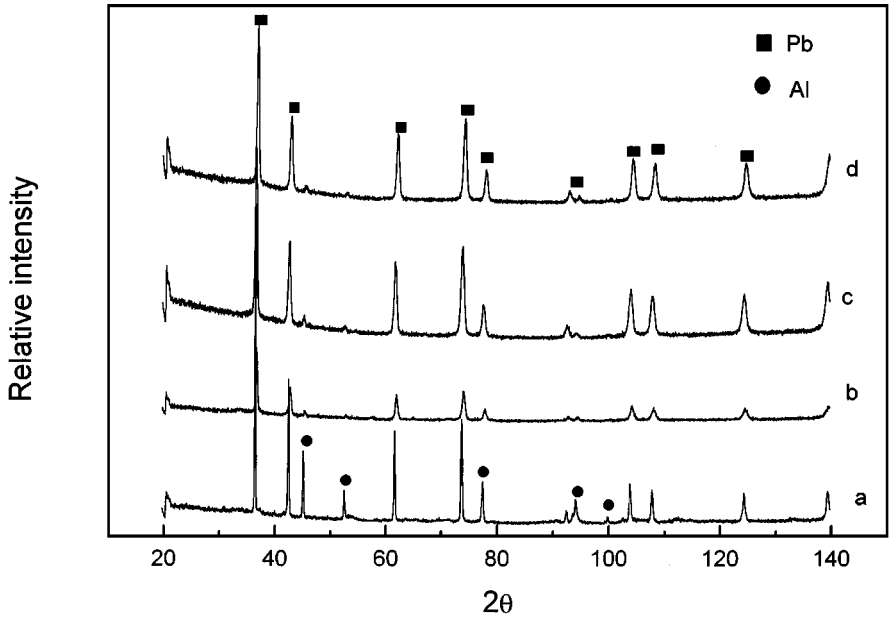

Figure 1 X-ray diffractograms of Pb-50% Al milled for different times. (a) 0, (b) 0.5 (c) 5 and (d) 15 h.

On the other hand, with regard to the solubility of supersaturated solid solution, it has been pointed out that only some of the solute atoms are dissolved into the lattice of the solvent as substitutional atoms and the rest are segregated to the boundary regions as atomic clusters and grain boundary atoms [15]. Therefore, the actual solubility is much lower than that derived from the nominal composition of powder mixtures in which only the solid solution phase is detected by X-ray diffraction analysis. Further work is required to get full understanding for the mechanism of the formation of supersaturated solid solution by MA.

Pb and Al are two components virtually immiscible in both solid and liquid states except at very high temperatures. Recently, it was reported that nanophase composite can be synthesized by MA of Pb-Al [16]. It is still not clear, however, if supersaturated solid solution has been formed. Unlike Ag-Cu [7, 17] and Fe-Cu [9, 18] in which supersaturated solid solution have been obtained by both rapid quenching and MA; the alloys obtained in the Pb-Al binary system by conventional solidification and rapid solidification are mixtures of pure Pb and Al [19, 20]. Thus, it is interesting to investigate the MA of Pb and Al to see if any alloy phases can be formed and to characterize the microstructure of alloy prepared by MA in the Pb-Al system, which has strong sedimentary tendency due to mutual immiscibility and big density difference between the components.

2. Experiment

Pure Al and Pb powders of 200 mesh size were used in this work and the purity of powders was 99.95%. 10 g powder mixtures of selected compositions were sealed in a stainless steel vial together with steel balls and milled in a Spex 8000 mill. The ratio of powder to ball was 1 : 5. Seven balls of 10 mm in diameter and 25 balls of 6 mm in diameter were used. The whole milling process was performed inside a glove box filled with high purity argon. The temperature inside glove box was always kept below 323 K. A planetary ball mill was also used and similar result was obtained. The structural variation of powders milled for different times was examined by X-ray diffraction. The lattice constant, grain size and atomic-level strain (root mean square) of the milled powders were determined by analyzing data of X-ray diffraction using the method described in [21]. A JEOL 840-SSD SEM attached with EDX accessory was used to observe the microstructure and composition distribution of as milled powder. The SEM sample was made by embeding the as milled powder in epoxy and grinding it. Since some particles obtained after milling were very coarse (several millimeters in diameter) due to the fact that Pb is very soft, thin foils were made directly from them. First, the coarse particle was ground to thin slab on sand paper, then further thinned to thin foil by ion milling. TEM and HREM investigation were performed in a CM-200. The composition of phases was analyzed by energy dispersive X-ray spectroscopy (EDX) accessory of H-9000 TEM. A PE PC series DSC7 Differential Scanning Calorimetric (DSC) was used to follow the heating process of the milled powder.

3. Results and discussion

3.1. Structural variation of Pb-Al powder mixture during MA

The structural variations of Pb-Al powder mixtures of different composition, e.g. Pb-33 at % Al, Pb-50 at % Al, Pb-75 at % Al and Pb-90 at % Al, after milling have been studied by X-ray diffraction. Fig. 1 shows the X-ray diffractogram of Pb-50 at % Al powder mixture milled for different times. It can be seen from Fig. 1 that the diffraction intensity of Pb increases and that of Al decrease significantly at the initial stage of milling. A steady state appears to have been reached after about 10 h of milling. From the X-ray diffraction result, it seems that the amount of phase with the structure of Pb increases while the amount of phase with the structure of Al decreases. The X-ray diffraction results of all milled Pb-Al powder mixtures are similar to that

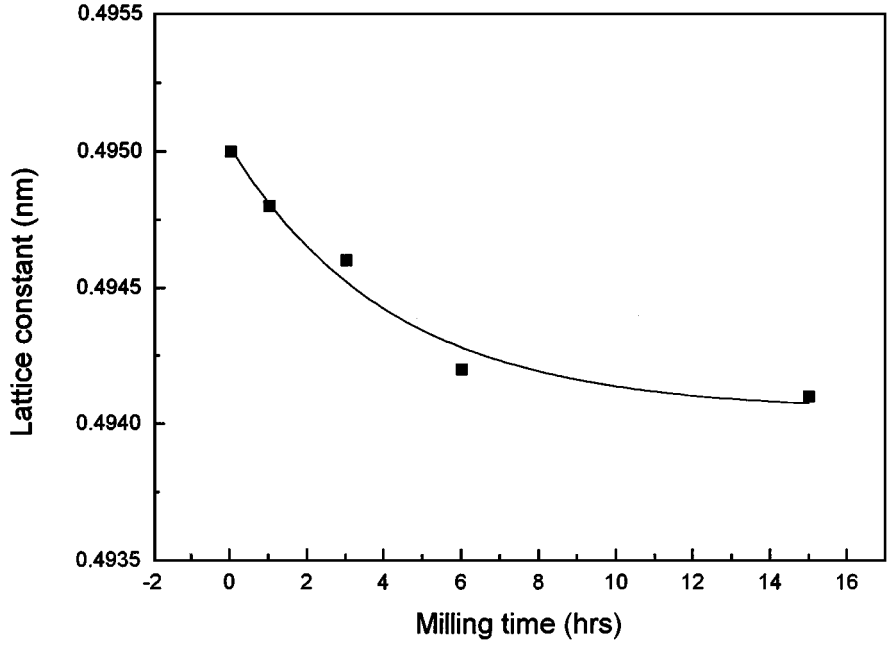

Figure 2 The dependence of lattice constant of Pb on the milling time measured in Pb-50 at % Al milled powder mixture.

shown in Fig. 1, and the common feature of them is that the diffraction intensity changes most markedly at the beginning stage of milling (within about 3 h). The relative diffraction intensity of Pb increases with a concomitant decrease in the diffraction intensity of Al. It can also be noticed that the diffraction peaks of Al and Pb are broadened but those of Al broadened much more apparent than those of Pb, which means that the grain size of Al and Pb is refined but the refining is much more significant for Al.

The intensity variation of X-ray diffraction pattern of milled Pb-Al powder must have been resulted from some microstructural changes caused by milling. There are two possible reasons. One is that the Al is dissolved into the lattice of Pb and a supersaturated solid solution is formed. Another important factor which should be taken into account in this system is that Pb absorbs X-ray strongly. Since Pb is much softer than Al, it is possible that Al powder is surrounded by Pb during milling. In this case, the X-ray beam incident to Al particles is greatly weakened and the diffraction beam from Al is also weakened. This effect can be quantitatively estimated approximately by using the equation relating the intensities of transmitted and incident beams as below:

$$I = I_0 e^{-(\mu/\rho).\rho.d} \tag{1}$$

Where I and I_0 are intensities of transmitted and incident beams, respectively, μ/ρ is mass absorption coefficient. ρ is the density of materials and d is the thickness of materials. In the case that the intensity of transmitted beam reduces to 10% of that of the incident beam by Pb, d is about 6 μm after substituting relevant values. However, this is only the transmission case. With regard to the diffraction intensity of Al, only half of the above thickness would reduce its intensity to 10% of the original value because both incident beam to Al and diffracted beam out of Al pass through the Pb surrounding it. Thus, the absorption effect of Pb may play an important role for the change of diffraction intensities of the milled powder. However, it is not clear merely from the intensity variation of X-ray diffraction peaks whether the dissolution of Al into Pb takes place and also contributes to the variation of diffraction intensities of the milled powder.

In order to check if the dissolution of Al into Pb has taken place during MA, the lattice constant of Pb has been carefully measured in accordance with the milling time in Pb-50 at % Al powder mixture in which the Al peaks nearly disappeared after 10 h milling. The result is shown in Fig. 2. It can be seen that the lattice constant of Pb reduces slightly. It is likely that some Al has dissolved into the lattice of Pb. However, the change in lattice constant should be much bigger if the amount of Al dissolved into Pb is consistent with the nominal composition of the powder mixture because the atomic size ratio of Pb to Al is about 1.22. If the Vegard's law is obeyed, only 1 at % of Al's dissolution into Pb should cause the change of lattice constant observed. Based on this result it is suggested that if there is a dissolution of Al into Pb, the amount should be small. Therefore, the surrounding of Al by Pb, resulting in the absorption of X-ray reaching and coming out of the Al as discussed above, should be the major factor responsible for the large decrease in the diffraction intensities of Al peaks.

3.2. Microstructure of milled Pb-Al powder

Microstructural feature of mechanically alloyed Pb-Al was analyzed by SEM and TEM on the Pb-50 at % Al sample milled for 10 h. Fig. 3 is a SEM micrograph showing the morphology of powder obtained by milling. The microstructure consists of two parts. One is bright chain-like structure and the other, which is the dominant part, is a homogeneous mixture of very fine phases. Results of EDX composition analysis of the samples are given in Table I. It can be seen that the average composition of sample is coincident with the

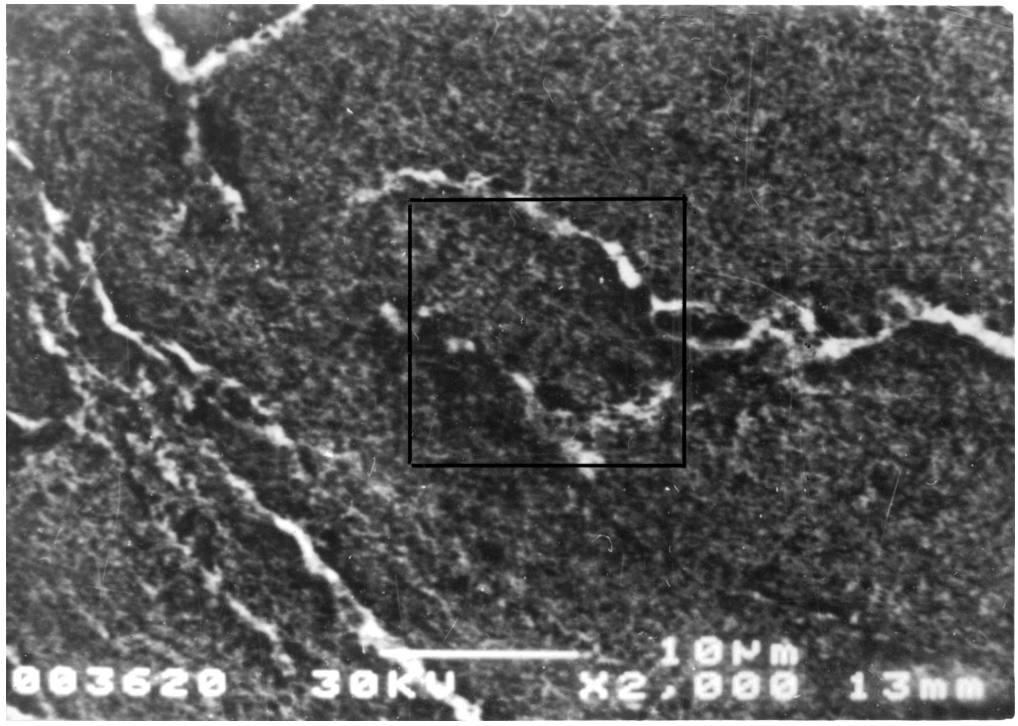

Figure 3 SEM micrograph of Pb-50 at % Al specimen milled for 10 h.

TABLE I EDX composition analysis of Pb-50 at % Al milled for 15 h (at %)

	Composition		
No	Pb	Al	Area measured
1	49.4	50.6	large area
2	96.3	3.7	bright region
3	93.8	6.2	bright region
4	87.5	12.5	bright region
5	66.1	33.9	matrix region
6	65.7	34.3	matrix region
7	66	34	matrix region

nominal composition of original powder mixture. However, the constituent of chain-like structure is mainly Pb. On balance, the Al concentration of the matrix is higher than the average composition of powder mixture. The matrix is composed of homogeneously distributed Pb and Al phases and the details will be shown in the TEM results. The SEM observation shows that the microstructure of milled powder is homogeneous and fine. Although there is a chain-like Pb rich structure, it is also not very coarse and is distributed homogeneously. It is expected that the chain-like product could be finally eliminated by prolonging the milling process. Therefore, homogeneous blending of Pb and Al can be easily achieved by mechanical alloying despite of their mutual immiscibility and strong sedimentary tendency due to the large difference in their density.

Fig. 4a is a TEM micrograph showing the microstructure of the Pb-50 at % Al sample milled for 10 h. Fig. 4b is the diffraction pattern corresponding to Fig. 4a. The indexing of this diffraction pattern proves that the microstructure shown in Fig. 4a is composed of two phases corresponding to Pb (dark region) and Al (bright region). It is evident that both of the phases are fine and homogeneously distributed. Fig. 5a shows a morphology obtained and it can be considered as a core surrounded by the matrix. Fig. 5b and c are diffraction patterns obtained in the region indicated by single and double arrows in Fig. 5a, respectively. The indexing of Fig. 5b confirms that the lattice of the matrix is coincident with that of Pb. Fig. 5c is a composite diffraction pattern of the matrix and the dark particle. By using dark field imaging and indexing the diffraction pattern, it was confirmed that the particles produced the diffraction pattern of Al. It can also be seen from Fig. 5c that Pb and Al phase are in cubic to cubic orientation relationship.

Examining Fig. 4a carefully, it can be seen that there are very fine particles inside the grains of Al phase. These particles are only about 10 nm in size (the smaller ones are only several nanometers). HREM and micro-diffraction analysis were used to identify these particles. Fig. 6a is a HREM image showing the small particles in Al grains. Diffraction analysis indicated that the small particles are Pb phase and they are in cubic to cubic orientation relationship with Al matrix. All particles inside one grain have the same crystallographic orientation. Fig. 6b is a [1 1 2] zone composite diffraction pattern of small particles and matrix obtained by micro-diffraction showing the cubic to cubic orientation relationship between the small particles and the matrix. It can also be noted that Moiré fringes present due to the impose of small particles with matrix. Due to the particle and matrix are in cubic to cubic orientation relationship, it is also convenient to determine the structure of particles and matrix by analyzing the HREM image and related Moiré fringes. In the present case spacing D of the Moiré fringe is related to spacing

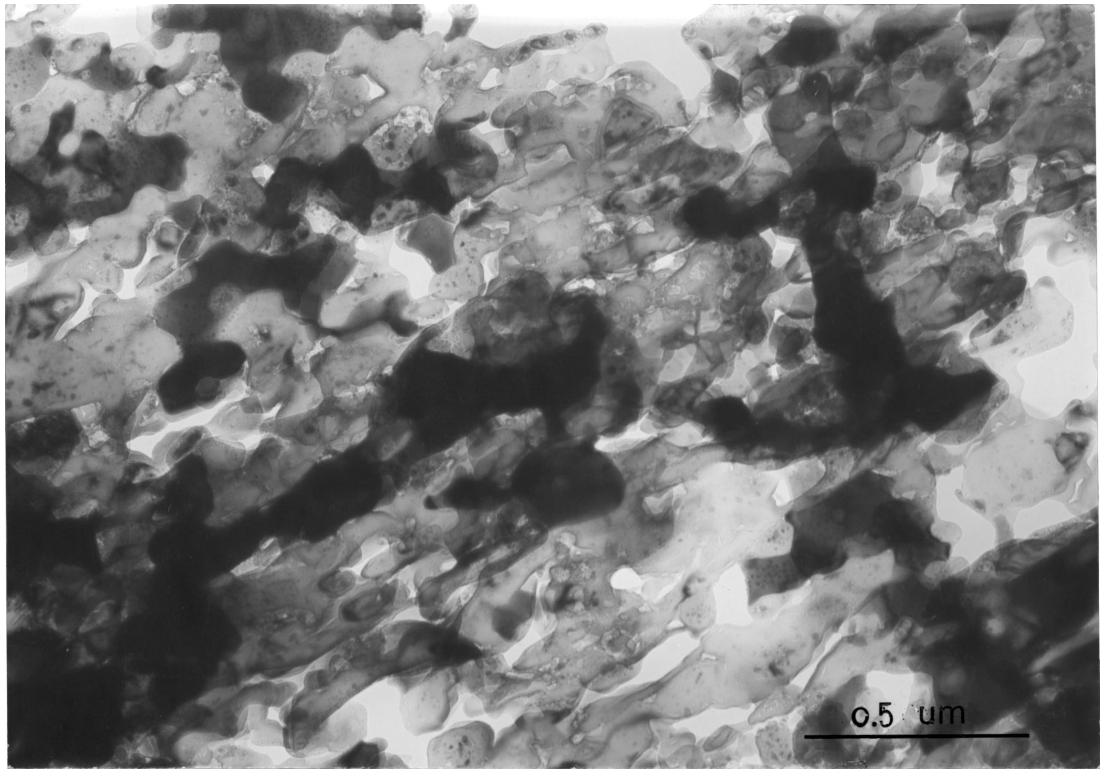

(a)

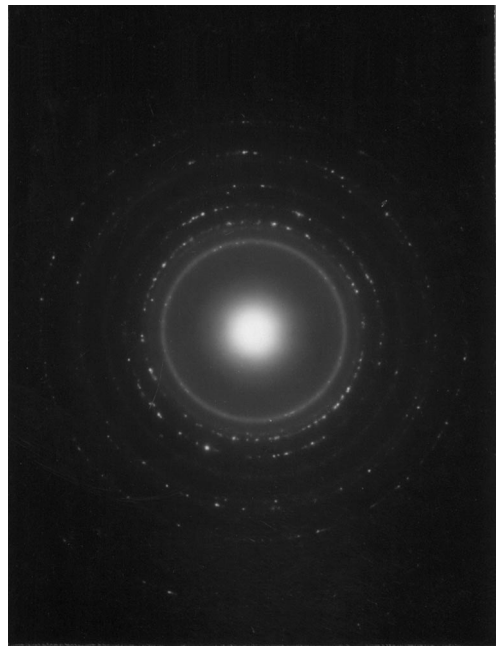

(b)

Figure 4 (a) TEM morphology of Pb-50 at % Al milled for 10 h. (b) Diffraction pattern corresponding to Fig. 4a.

of lattice plane of Al and Pb (d_{Pb} and d_{Al}) of the same (hkl) as below:

$$D = 1/(1/d_{Al} - 1/d_{Pb}) \quad (2)$$

Substituting standard data of Al and Pb, we have

$$D = 5.54d_{Al} \quad \text{or} \quad D = 4.54d_{Pb} \quad (3)$$

Using this relation the particles and matrix were identified to be Pb and Al respectively and is coincident with the diffraction analysis.

Based on above TEM and HREM observation, the microstructure of ball-milled Pb-Al could be characterized. For Al phase its grain size is greatly refined to less than about 200 nm and many of the Al grains are less than 30 nm. For the Pb phase its grain size is larger than that of Al. However, there are very fine Pb particles of about 10 nm distributed homogeneously inside the larger grains of Al, and the orientation relationship between these small Pb particles and Al matrix is cubic to cubic. In addition, the Al and Pb phase are homogeneously blended. Thus, a composite structure containing nanometer sized Pb and Al phases was obtained.

Fig. 7a and b are EDX spectra obtained in region of single phase with lattice structure of Pb and Al, respectively. It is interesting that there is a small amount of Al and Pb in regions with structure of Pb and Al, respectively. This provides further evidence for the formation of supersaturated solid solution, although accurate quantitative analysis was not obtained. However, It should be pointed out that fine particles of Pb may make contribution to the Pb peak in EDX spectroscope obtained in region of single Al phase or vice versa although the area of EDX measurement was carefully chosen to exclude the fine particles. This is because that distribution of fine particles of Pb in Al or vice verse is dense and disperse.

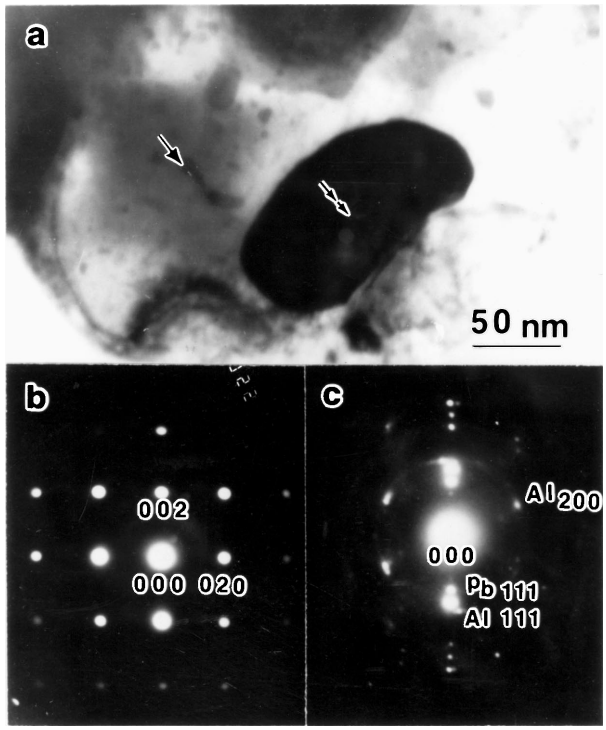

Figure 5 The morphology and selected area electron diffraction (SAD) pattern of Pb-50 at % Al milled for 10 h: (a) morphology, bright field image, (b) SAD pattern ([0 1 1] direction of Pb) taken at region indicated by single arrow and (c) SAD pattern ([0 1 1] direction of Al) taken at region indicated by double arrow.

3.3. Effect of heating on the mechanically alloyed Pb-Al powder

Fig. 8 is a DSC trace of Pb-50 at % Al ball-milled powder. The powder had been milled for 10 h. The sharp endothermic peak at 593 K corresponds to the melting of lead. There is also an exothermic peak which spans a wide temperature range from 373 to 490 K approximately. The ΔH of this peak is about 6.93 J/g. As it is known, the precipitation of secondary phase from supersaturated solid solution results in an exothermic peak during the heating of supersaturated solid solution in a DSC scan [22]. The supersaturated solid solution formed by MA must be in a non-equilibrium state and transform to the equilibrium state if suitable kinetic condition is provided. Therefore, decomposition process of supersaturated solid solution to pure Pb and Al phases was expected when it was heated. This decomposition makes contribution to the exothermic peak in DSC curve. On the other hand, however, the stored energy of mechanically alloyed materials kept in the form of lattice defects, strain and/or increased grain boundary area was released during heating and resulted in a wide exothermic peak in trace of DSC scan [23, 24]. From the microstructure observation described

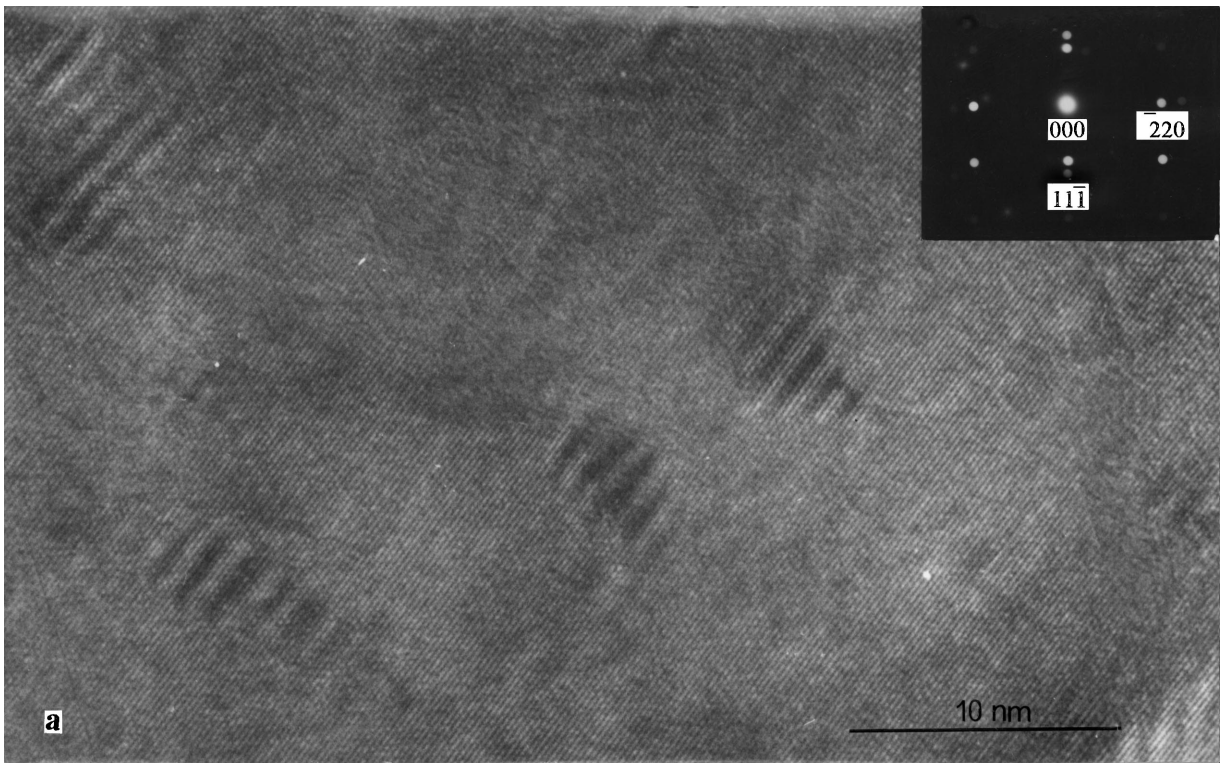

Figure 6 HREM image of Al grain containing nanometer sized Pb particles (a) and [1 1 2] composite diffraction pattern of Al matrix and small Pb particles showing cubic to cubic orientation relationship between them (b).

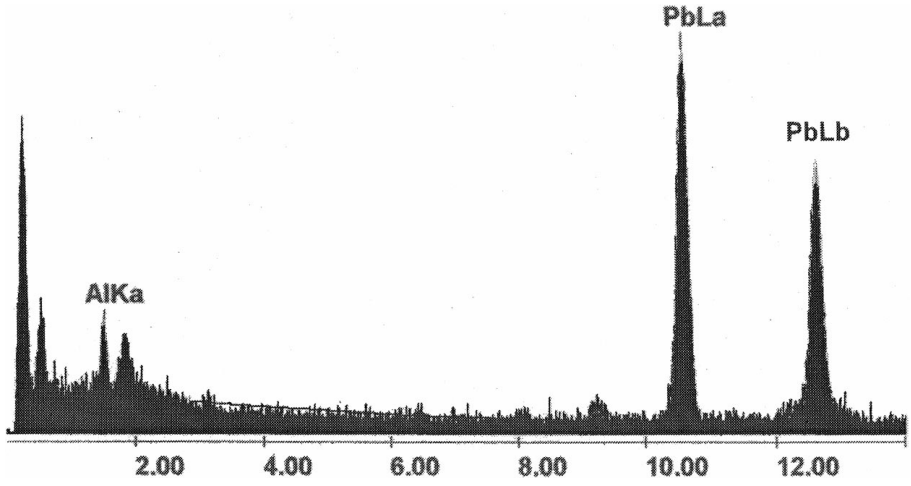

(a)

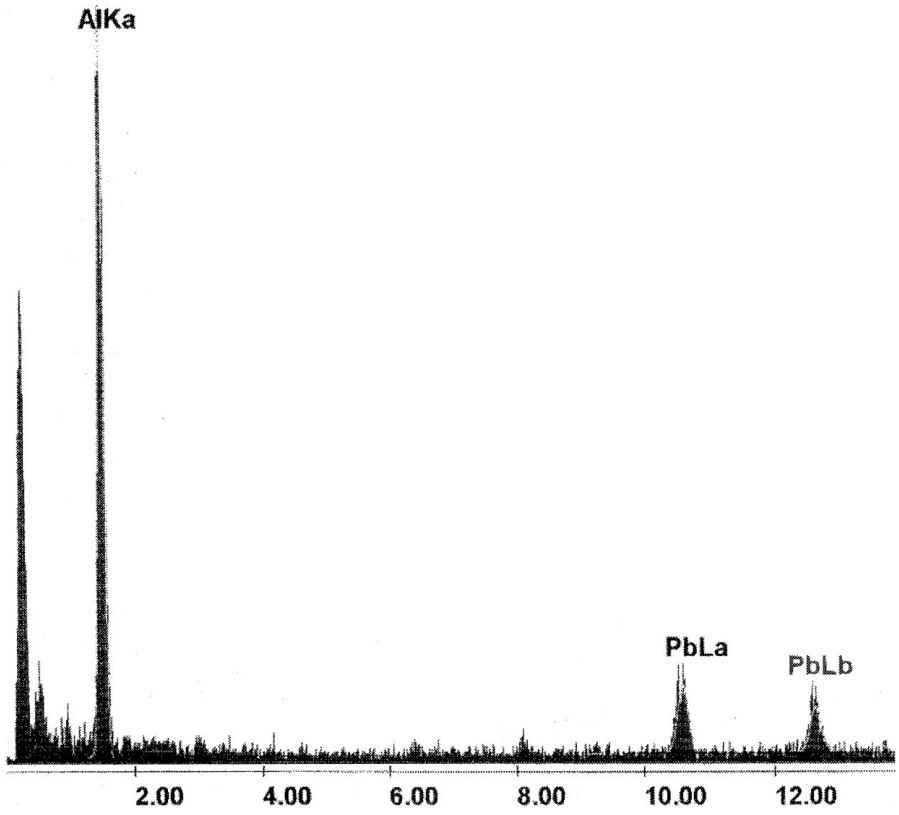

(b)

Figure 7 EDX spectrums obtained at the region with lattice structure of Pb (a) and of Al (b).

previously, nanocrystallined structure was formed in Pb-Al mixture by ball milling. Therefore, it seems that both decomposition of supersaturated solid solution and the release of energy stored contributed to the exothermic peak shown in Fig. 8.

3.4. Discussion

The experimental results show that the microstructure of Pb-Al obtained by MA is homogeneous and disperse. However, it is somewhat different from that observed in the nanocrystalline pure metals formed by MA [3]. As milling proceeds, the grain size of Al decreased and the dependance of average grain size on milling time derived from X-ray diffraction was given in Fig. 9. The grain size of Al decreased to about 30 nm after milled for 15 h. On the other hand, however, Pb phase exists in two dimension levels, respectively. For the larger scale the Pb grains of less than about 0.5 μm are mixing homogeneously with Al grains. For the smaller scale very fine Pb particles of about 10 nm distribute inside Al grains. In general, it is accepted that the nanocrystalline formation by MA evolves from dislocation cell structures within shear bands [3]. By further deformation, the dislocation cells/low-angle grain boundaries vanish, leading finally to a fully nanocrystalline powder with a completely random orientation of neighbouring grains separated by high angle grain boundaries [3]. The final grain size achieved by MA is governed by plastic deformation via dislocation motion and the rate

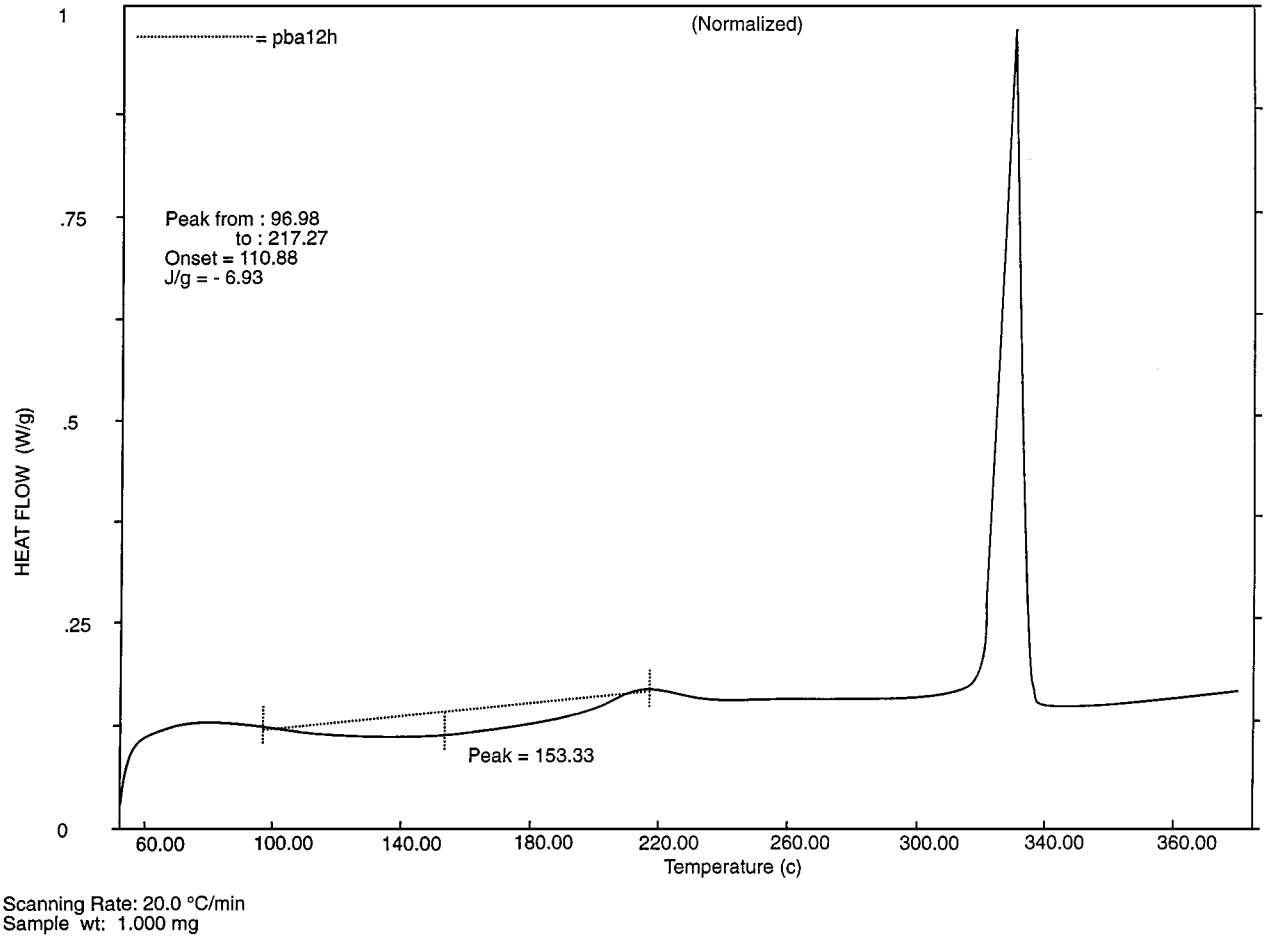

Figure 8 DSC trace of heating scan for Pb-50 at % Al powder milled for 10 h.

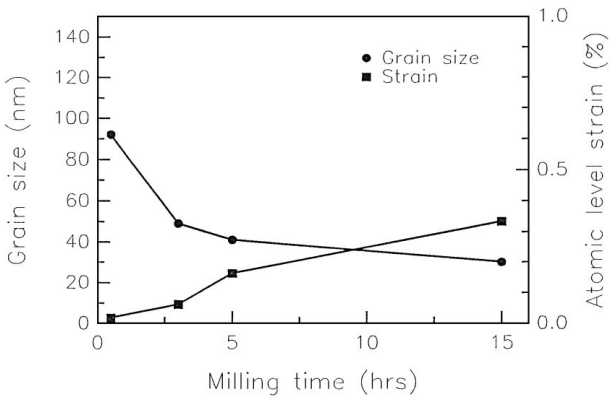

Figure 9 The dependence of average grain size and atomic level strain of Al on the milling time measured in Pb-50 at % Al milled powder.

of recovery during milling [25]. It is likely that the refinement of Al phase to nanometer size is still observe the dislocation mechanism. With regard to the Pb phase, dynamic recovery takes place during the deformation process of milling because that melting point of Pb is only 600 K and ball milling results in certain temperature rise (100–300 K [26]). Therefore, nanocrystalline could not evolve from multiplication of dislocations and the grain size of Pb phase is quite coarse. In this sense, the presence of nanometer sized Pb particles inside Al grains could not be explained using the dislocation multiplication mechanism. Other mechanism should be considered. On one hand, as mentioned before, supersaturated solid solution was probably formed in Pb-Al system by MA. On the other hand, however, the supersaturated solid solution formed is metastable and tends to decompose to Al and Pb subsequently for there is a steady temperature rise inside milling vial which is favorable to the decomposition of supersaturated solid solution. As a result, small particles of Al and Pb precipitate from Pb and Al in a cubic to cubic orientation relationship. It is probably like that there is a dynamic balance between formation of supersaturated solid solution and precipitation of small Pb particles.

The formation of supersaturated solid solution by MA has been reported in several different cases. Sui *et al*. reported that the solubility of AlCo intermetallic compound can be greatly enhanced by MA and it was suggested that the extra solute atom segregates at boundary regions of nanocrystalline AlCo phase. So, it is a solution on nanoscale [5]. In the case of immiscible Fe-Cu system, it was reported that Cu could dissolve into the lattice of Fe or vice versa [9]. The driving force for the formation of supersaturated solid solution in Fe-Cu has been attributed to several aspects, such as capillary pressure of fine particles [13] and the existence of stress fields of dense dislocations induced by milling [14]. In the case of Pb-Al in this work, TEM and HREM observation reveals that there is no high density of dislocation in the as-milled powder. On the other hand, upon grinding the components milled were

continuously fragmented. Consequently, small fragments of Pb and Al were generated. The capillary pressure of these small fragments may provide a driving force, as described by Gibbs-Thomson equation, for the dissolution in Pb-Al immiscible system. Based on this consideration and experiment results it is suggested that supersaturated solid solution has been formed in Pb-Al system. However, the solubility should be very low although accurate result have not been obtained yet.

4. Conclusions

In the present work, Pb-Al powder mixtures of different ratios have been ball milled. X-ray diffraction, TEM, HREM and EDX analysis show that homogeneous blending of Pb and Al can be achieved by MA despite their mutual immiscibility and large difference in density. The microstructure of the milled Pb-Al is nanocrystalline Al particles and microcrystalline Pb particles distributed homogeneously. There are also very fine Pb particles of about 10 nm inside coarse Al grains. By lattice constant measurement, TEM and DSC analysis, it has also been demonstrated that supersaturated solid solution was formed by MA. The increment of free energy due to the large increase in surface area caused by the formation of small fragments of component to nanoscale probably provides the driving force for the formation of supersaturated solid solution.

Acknowledgements

This research was partly supported by National Natural Science Foundation of China under contract No. 59541008. The authors would like to thank Drs. H. X. Sui and X. F. Duan of the Beijing Laboratory of Electron Microscopy for their assistance in EDX analysis. One of the authors (M. Z) is grateful to the Croucher Foundation for the financial support for his visit to the City University of Hong Kong.

References

1. A. Y. YERMAKOV, Y. Y. YUCHIKO and V. A. BARINOV, *Phys. Met. Metall.* **52** (6) (1981) 50.
2. C. C. KOCH, O. B. CAVIN, C. G. MCKAMEY and J. O. SCARBROUGH, *Appl. Phys. Lett.* **43** (1993) 1017.
3. H. J. FECHT, in "Nanophase Materials," edited by G. C. Hadjipanayis and W. Siegel (Kluwer Academic Publisher, 1994) p. 125.
4. H. J. FECHT, G. HAN, Z. FU and W. L. JOHNSON, *J. Appl. Phys.* **67** (1990) 1744.
5. H. X. SUI, M. ZHU, M. QI, G. B. LI and D. Z. YANG, *J. Appl. Phys.* **71** (6) (1992) 2945.
6. Y. L. CHEN, M. ZHU, M. QI, D. Z. YANG and H. J. FECHT, *Materials Science Forum*, **179–181** (1995) 133.
7. K. UENISH, K. F. KOBAYASHI, K. N. ISHIHARA and P. H. SHINGU, *Mater. Sci. Eng.* **A134** (1991) 1342.
8. E. IVANOV, *Material Science Forum*, **88–90** (1992) 475.
9. K. UENISHI, K. F. KOBAYASI, S. NASU, H. HATANO, K. ISHOHARA and P. H. SHINGU, *Z. Metallkd.* **83** (1992) 2.
10. M. ZHU and H. J. FECHT, *Nanostructured Mater.* **6** (1995) 921.
11. E. MA, M. ATZMON and P. E. PINKERTON, *J. Appl. Phys.* **74** (2) (1993) 955.
12. U. HERR, J. JING, U. CONSER and H. GLEITER, *Solid State Commun.* **76** (1989) 197.
13. A. R. RAVAYI, P. J. DESRE and T. BENAMEUR, *Phy. Rev. Lett.* **68** (14) (1992) 2235.
14. J. ECKERT, J. C. HOLZER, C. E. KRILL and W. L. JOHNSON, *J. Appl. Phys.* **73** (6) (1993) 2794.
15. J. Y. HUANG, A. Q. HE and Y. K. WU, *Nanostructured Materials* **4** (1) (1994) 1.
16. M. ZHU, B. L. LI, Y. GAO, L. LI, K. C. LUO, H. X. SUI and Z. X. LI, *Scripta Materialia* **36** (1997) 443.
17. P. DUWEZ, R. H. WILLENS and W. KLEMENT JR., *J. Appl. Phys.* **31** (1960) 1136.
18. W. KLEMENT, JR., *Trans. AIME.* **233** (1965) 1180.
19. K. I. MOORE, D. L. ZHANG and B. C. CANTOR, *Acta Metall.* **38** (1990) 1327.
20. J. F. COLE and F. E. GOODWIN, *J. Metals* **42**(6) (1990) 41.
21. H. P. KLUG and L. ALEXANDER, "X-Ray Diffraction Procedures for Polycrystalline and Amorphous Materials," 2nd edition (Wiley, New York, 1974).
22. M. VON. ROOYEN and E. J. MITTEMEIJIER, *Metall. Trans.* **20A** (1989) 1207.
23. T. OHASHI and Y. TANAKA, *Mater. Trans. Jap. Inst. Met.* **32** (1991) 587.
24. H. J. FECHT, E. HELLSTERN, Z. FU and W. L. JOHNSON, *Metall. Trans.* **21A** (1990) 2333.
25. J. ECKERT, J. C. HÖLZER, C. E. KRILL and W. L. JOHNSON, *J. Mater. Res.* **7** (1992) 1751.
26. J. ECKERT, L. SCHULTZ, H. HELLSTERN and K. URBAN, *J. Appl. Phys.* **64** (1988) 3224.

Received 22 April 1988
and accepted 14 September 1998